Hopping Transport of Electrons via Si-Dot

H. Watanabe

Advanced LSI Tech. Labs., Toshiba Corporation, Isogo, Yokohama 235-8522, Japan
pierre.watanabe@toshiba.co.jp

Abstract

We clarify the mechanism of single electron hopping and demonstrate single electron ocsillation via Si-dot, using a high-presice general-puprpuse device-simulator.

1 Introduction

Aggressive scaling of non-volatile memory (NVM) cells is going to replace floating gate by Si-dots. In this case, the injection or the emission of a few electrons significantly affects on the potential profile around the Si-dot, which means that the operation of such an NVM cell is quite sensitive to several electrons stored in the Si-dot. As schemed in the left hand of Figure 1, just after an electron is injected to the Si-dot, the Si-dot is upward in energy-band diagram. Then, the electric field across the first oxide (oxide-1) beneath the Si-dot is decreased while that across the second oxide (oxide-2) above the Si-dot is increased. (The structure is schemed in the right-hand.) This increases the emission rate from the Si-dot to the gate poly-Si and decreases the injection rate from the Si-substrate to the Si-dot. In opposite, the electric fields across the oxide-1 and across the oxide-2 are increased and decreased, respectively, just after an electron is emitted from the Si-dot to the gate poly-Si. Then, the emission rate is decreased and the injection rate is increased. In such a way, the potential shift by an electron may break the detailed balance condition that the rates of injection and emission are the same. In this work, we carry out the highly-precise device-simulation to analyze a potential fluctuation by an electron, and then clarify the mechanism of hopping transport via Si-dot.

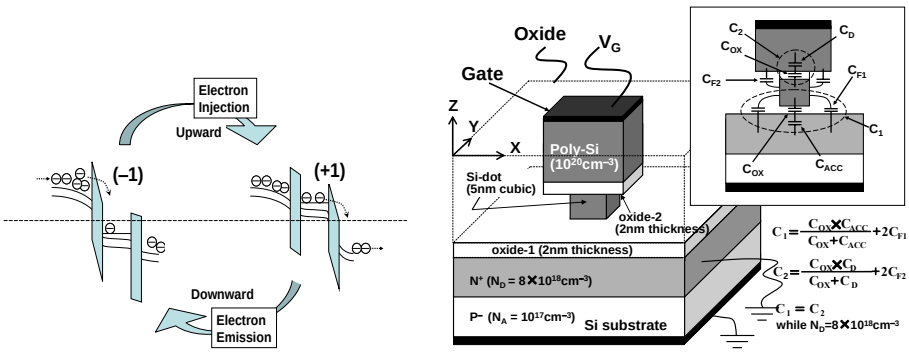

Figure 1: The left-hand figure is a scheme of hopping transport via Si-dot: The dashed line is a guide for the eyes, indicating that the Si-dot of (+1) is at higher level in energy band diagram than that of (–1). The right-hand is the structure of calculated sample: We have set $N_D=8\times10^{18}cm^{-3}$ such that $C_1 = C_2$ because C_{F1} is larger than C_{F2}.

2 Calculation

From the above-mentioned view point, we consider the sample structure of 5nm-cubic Si-dot, shown in Figure 1. The donor concentration of the diffusion layer is $8\times 10^{18}cm^{-3}$, in which case the capacitances of the oxide-1 and the oxide-2 are the same ($C_1 = C_2$). We use the tunnel mass of $0.85m_0$, where m_0 is the rest electron mass, considering the influence of the interfacial transition (IFT) layer in which the band gap and the dielectric constant changes from Si to pure oxide (SiO_2), according to x=1 to 0 in $(Si)_X - (SiO_2)_{1-X}$ [1]. Since the surface potential significantly affects on the electric field across the oxide-1 facing the Si-surface, we also have to consider the influence of the IFT layer on the surface quantization in the accumulation layer. We then add the IFT layer to the distance from the Si-surface as an argument of quantum correction potential of the simplified density-gradient method [2] that is used in this work. Further, we consider the depletion layer of gate poly-Si with the surface band-gap narrowing as well as the bulk bang-gap narrowing [3]. We use the calculation method of 3-dimensional tunnel current (published in [4]) to calculate the rate of injection and emission. We also consider the eigenstates quantum-mechanically split inside the Si-dot and the coulomb blockade potential. We successfully implement all the above mentioned models into the general-purpose device-simulator, and then carry out a fully self-consistent device-simulation at room temperature.

3 Results and Conclusions

In order to confirm the precision of the present method, we calculate the number of electrons stored in 100 nm cubic floating gate in which there are ten-million donor ions (i.e. $10^{20}cm^{-3}$). Figure 2 show that it reaches the discrepancy between the surface charges of the oxide-1 and the oxide-2 over 300 iterations. This means that the relative error is at most 0.001% in this test calculation. In Figures 3-5, we show the calculation results of the 5nm-cubic Si-dot sample shown in Figure 1. As shown in the left-hand of Figure 3, the potential of the Si-dot is increased up to 8 μsec as the input pulse (V_G) is increased over time. At 8 μsec, the one-by-one step injection starts, then suppressing the increase of the Si-dot potential and causing the plateau from 8 to 14 μsec in Figures 3-5. Further, the saturation of the injection is shown at 14 μsec in these figures, after which we have an oscillation due to the cyclic rotation of injection-emission schemed in Figure 1. Although V_G is fixed after 20 μsec, this oscillation is left. From the insertions of Figure 3, the potential shift by an electron is estimated 250 mV from (4-3) V / (9-5), which value is much larger than thermal energy at room temperature (≅26 meV), then breaking the detailed balance condition that the rates of injection and emission are the same. In Figure 4, it is shown that the electric fields across the oxide-1 and the oxide-2 are almost same before 8 μsec. This is because we have set the sample structure such that $C_1 = C_2$, in order to study the influence of injection. After 8 μsec, the electric field across the oxide-1 is indeed apart from that across the oxide-2, which is clearly due to the one-by-one step injection. By this way, the stored electrons decrease the Si-dot potential from that determined by the capacitance coupling ratio, $Cr = C_2 / (C_1 + C_2)$. The amount of this decrease divided by Cr would be V_{TH}-shift by programming if we considered an NVM cell. Figure 5 depicts the calculated fluxes that are defined as an expected

number of injected and emitted electrons per a second. Before 8 μsec, the flux through the oxide-2 (emission flux) is negligible because no stored electrons in the Si-dot, while that through the oxide-1 (injection flux) is increased over time with V_G owing to many electrons in the accumulation layer at the Si-surface. After the injection starts at 8 μsec, the emission flux (oxide-2) is increased over time and catches up the injection flux (oxide-1), then reaching a saturation state at 14 μsec. In the right hand side, after 20 μsec, we have an iterative turnover of emission-injection, in which phases are different by half cycle. This phase difference exhibits an iterative charge-pumping process in the Si-dot. Since the fluxes of injection and emission are proportional to the substrate and the gate currents, respectively, electrons transport from the substrate to the gate step-by-step via the Si-dot. Therefore, the cyclic rotation of injection-emission causes the hopping transport of electrons via Si-dot.

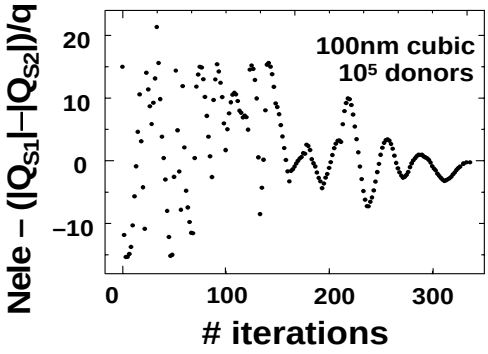

Figure 2: The numerical error: Nele is the number of stored electrons, Q_{S1} and Q_{S2} are the surface charges of the oxide-1 and the oxide-2, respectively. The q is the elementary charge.

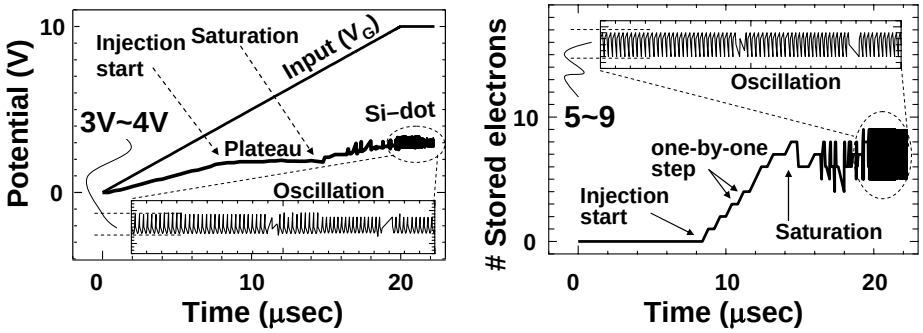

Figure 3: The left-hand depicts the calculated potential of Si-dot over time (measured from the initial state at which V_G is zero): The insertion is from the dashed circle. The righ-hand depicts the calculated numbers of stored electrons over time: The insertion is from the dashed circle.

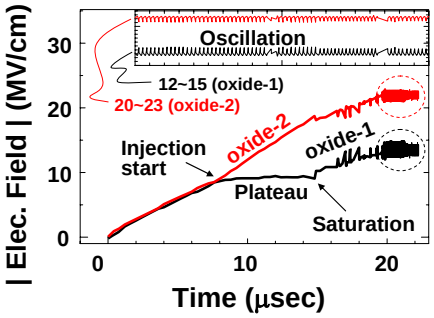

Figure 4: Electric field over time: The insertion is from the dashed circles.

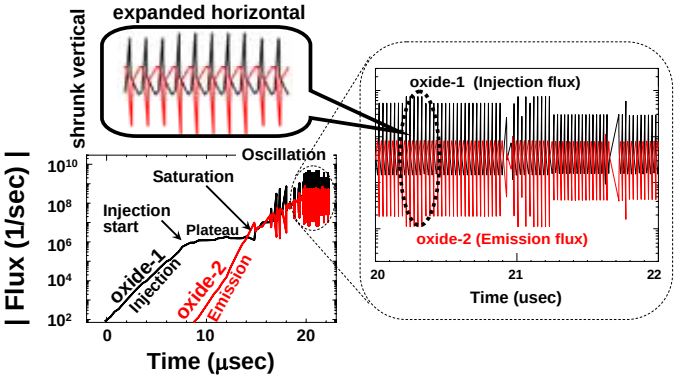

Figure 5: Flux over time and oscillation.

4 Summary

The present technique is applicable to single electron fluctuation. It is then demonstrated that the cyclic rotation of injection-emission causes the hopping transport via Si-dot. This technique is also applicable to study the hopping transport via local traps in dielectrics of CMOS devices and NVM cells.

References

[1] H. Watanabe, D. Matsushita, and K. Muraoka, "Determination of tunnel mass and physical thickness of gate oxide including poly-Si/SiO_2 and Si/SiO_2 interfacial transition layers", IEEE Trans. Elec. Dev., vol. 53, pp. 1323-1330, 2005.

[2] K. Matsuzawa, S. Takagi, M. Takayanagi, H. Tanimoto, "Device simulation of surface quantization effect on MOSFETs with simplified density-gradient method", Sold-State Elec., vol. 46, pp. 747-751, 2002.

[3] H. Watanabe, "Depletion layer of gate poly-Si", IEEE Trans. Elec. Dev., vol. 52, pp. 2265-2271, 2005.

[4] H. Watanabe, K. Matsuzawa, S. Takagi, "Scaling effects on gate leakage current", IEEE Trans. Elec. Dev., vol. 50, pp. 1779-1784, 2003.